

## Pseudoplane-wave gravitational calibrator for gravitational wave observatories

M. P. Ross<sup>1,\*</sup>, J. H. Gundlach<sup>1,†</sup>, E. G. Adelberger<sup>1</sup>, C. M. Weller,<sup>2</sup> E. A. Shaw,<sup>1</sup> C. Gettings<sup>1</sup>, J. Kissel<sup>3</sup>, T. Mistry,<sup>4</sup> L. Datrier,<sup>5</sup> E. Daw<sup>4</sup> and M. Hendry<sup>5</sup>


<sup>1</sup>*Center for Experimental Nuclear Physics and Astrophysics, University of Washington, Seattle, Washington 98195, USA*

<sup>2</sup>*California Institute of Technology, Pasadena, California 91125, USA*

<sup>3</sup>*LIGO Hanford Observatory, Richland, Washington 99352, USA*

<sup>4</sup>*The University of Sheffield, Sheffield S10 2TN, United Kingdom*

<sup>5</sup>*SUPA, University of Glasgow, Glasgow G12 8QQ, United Kingdom*

 (Received 25 January 2023; accepted 21 February 2023; published 6 March 2023)

The precisions of existing gravitational calibrators for gravitational wave observatories are limited by their dependence on the relative position between the calibrators and the observatory's test masses. Here we present a novel geometry consisting of four quadrupole rotors placed at the vertices of a rectangle centered on the test mass. The phases and rotation directions are selected to produce a pseudoplane-wave sinusoidal gravitational acceleration with amplitude of  $\sim 100$  fm/s<sup>2</sup>. We show that this acceleration only has minimal dependence on the test mass position relative to the rotor array and can yield 0.15% acceleration amplitude uncertainty while tolerating a 1-cm test mass position uncertainty. The acceleration can be directed precisely along the optical axis of the interferometer arm and applies no torque on the test mass. In addition, the small size of the rotors has significant engineering and safety benefits.

DOI: [10.1103/PhysRevD.107.062003](https://doi.org/10.1103/PhysRevD.107.062003)

### I. INTRODUCTION

Gravitational wave astronomy has blossomed into a novel method to observe the Universe. The number of gravitational wave observations is expected to grow substantially in the coming years with the continued operation of the LIGO [1] and Virgo [2] interferometers as well as the future addition of LIGO-India [3] and the further improvements of KAGRA [4].

Precise and robust absolute calibration of these interferometers is essential. Cosmological measurements [5–7], searches for deviations from general relativity [8], and binary-merger characterization [9] all require precise strain calibrations. Currently, these calibrations are made using photon pressure [10,11]. These calibration systems provide absolute calibrations limited to  $\sim 0.4\%$  uncertainty [12]. Improvements on this have proven difficult. In addition, relying on a single calibration system may be susceptible to unknown systematics.

Calibrating with a gravitationally induced strain has long been suggested as an alternative calibration technique [13–18] and has recently been implemented at gravitational wave observatories [19–22]. Gravitational calibration has

multiple advantages over photon pressure including minimal sources of systematic error and guaranteed stability over long time durations. Operating both gravitational and photon calibration systems allows the systems to cross-check each other and combined yield a higher-precision absolute calibration.

Single-rotor gravitational calibrators [19,21,22] produce accelerations that have large dependence on the radial distance  $r$  between the rotor and the test mass. The acceleration is typically proportional to  $\sim 1/r^{l+2}$  where  $l$  is the order of the dominant mass-multipole moment. For example, a rotor with a quadrupole mass distribution ( $l = 2$ ) will follow  $\sim 1/r^4$ . This strong positioning dependence causes the performance of the absolute calibration to be limited by the measurement of the test mass to rotor separation. The Virgo observatory is pursuing an asymmetric system of rotors rotating at different frequencies that may alleviate this limitation [20].

Here, we present a novel geometry consisting of four quadrupole rotors that produces a pseudoplane-wave gravitational acceleration; see Sec. IV. This symmetric geometry has no first-order dependence on the position of the rotors relative to the test mass. It instead depends on the easy-to-measure positions between the rotors in the array. Additionally, this geometry suppresses the torques acting on the test mass and eases much of the engineering and safety concerns of previous rotors.

\*mpross2@uw.edu  
†gundlach@uw.edu

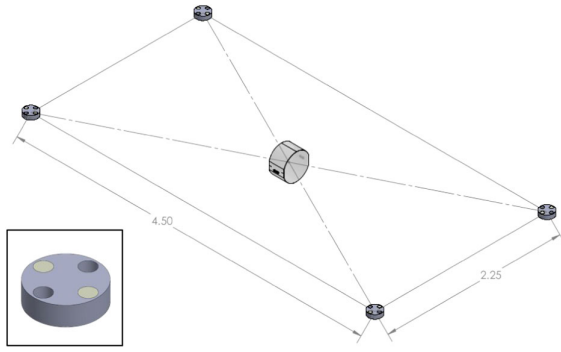


FIG. 1. A rendering of the geometry of the rotors with the test mass at the center of the 2.25-m by 4.50-m rectangle. Also shown is a detail of a single rotor consisting of the dark gray aluminum disk with two light gray tungsten slugs inserted into two of the four-rotor holes.

## II. GEOMETRY

The example pseudoplane-wave calibrator proposed here consists of four identical rotors placed at the vertices of a 2.25-m by 4.50-m rectangle centered on the test mass. Figure 1 shows a rendering of the geometry placed around LIGO’s end-station vacuum chamber. The rotors are designed with the similar dimensions as the LIGO Newtonian Calibrator (NCal) [22] but without a hexapole mass arrangement. Each rotor is a 17-cm-diameter, 5-cm-tall aluminum disk with four holes cut at a radius of 6 cm separated by 90°. Two holes are filled in with 4-cm-diameter, 5-cm-tall tungsten cylinders which produce a quadrupole mass distribution. The parameters of the geometry are displayed in Table I.

The rotor parameters that are common with the LIGO NCal are assigned uncertainties equal to what was previously achieved [22]. The rest of the parameters (positioning, phase, etc.) are assigned uncertainties based on what is reasonably achievable with standard measurement

techniques. For example, since the rotors would be outside the interferometer’s vacuum system, their positions can be readily measured to mm precision with standard surveying equipment [22].

The relative phases of the rotors and the rotation directions are set to achieve a pseudoplane-wave nature. The four rotors with a positive  $x$  coordinate are rotated by 90° from the rotors with a negative  $x$  coordinate. Additionally, the rotors with a positive  $y$  coordinate rotate clockwise, while those with negative  $y$  coordinates rotate counterclockwise. These choices cause the applied acceleration to be purely in the  $x$  direction with no net torques.

## III. ENGINEERING SIMPLICITY

Since the four-rotor array produces more acceleration at a given separation than a single rotor, the array can be placed at a larger radius to produce a similar amplitude acceleration on the test mass. This allows the array to be placed well away from the existing infrastructure of the observatories. Here we have chosen a geometry that fits around the LIGO end-station vacuum chamber and seismic isolation system, as shown in Fig. 2. This significantly simplifies the structure that holds the rotors, as it does not need to be incorporated into the existing structural components.

The use of only quadrupole mass distributions as compared to both quadrupole and hexapole masses [22] decreases the rotor’s kinetic energy thus decreasing the likelihood of damage through catastrophic failure. Because of the decreased moment of inertia, a smaller radius also decreases the torques needed to spin the rotor and maintain a fixed rotation speed which loosens the requirements on the drive motors as well as decreases spurious electromagnetic effects caused by the motors and auxiliary electronics.

TABLE I. Individual contributions to the acceleration uncertainty for the parameters of the simulation. The quadrature sum is only an approximation of the uncertainty. The full uncertainty must take into account nonlinearities and degeneracies as is done in Fig. 4.

Parameter	Mean	Estimated uncertainty	Fractional acceleration uncertainty
Cylinder mass	1 kg	0.3 g	$3.5 \times 10^{-4}$
Cylinder radius	2 cm	2.5 $\mu\text{m}$	$1.5 \times 10^{-8}$
Cylinder length	5 cm	5 $\mu\text{m}$	$2.7 \times 10^{-8}$
Quadrupole radius	6 cm	5 $\mu\text{m}$	$1.7 \times 10^{-4}$
Test mass <sup>a</sup>	40 kg	10 g	$1.9 \times 10^{-15}$
Test mass length	200 mm	0.1 mm	$4.0 \times 10^{-6}$
Test mass radius	170 mm	0.05 mm	$3.9 \times 10^{-6}$
Test mass flat width	327 mm	0.05 mm	$1.4 \times 10^{-15}$
Rotor positions	( $\pm 2.25$ m, $\pm 1.125$ m, 0 m)	(1 mm, 1 mm, 1 mm)	$1.1 \times 10^{-3}$
Test mass position	(0 m, 0 m, 0 m)	(1 cm, 1 cm, 1 cm)	$1.3 \times 10^{-4}$
Rotor relative phase	0°, 90°	1°	$1.2 \times 10^{-3}$
Quadrature sum			$1.68 \times 10^{-3}$

<sup>a</sup>Since the gravitational acceleration is independent of the test mass, this entry represents the numerical precision of the simulation.

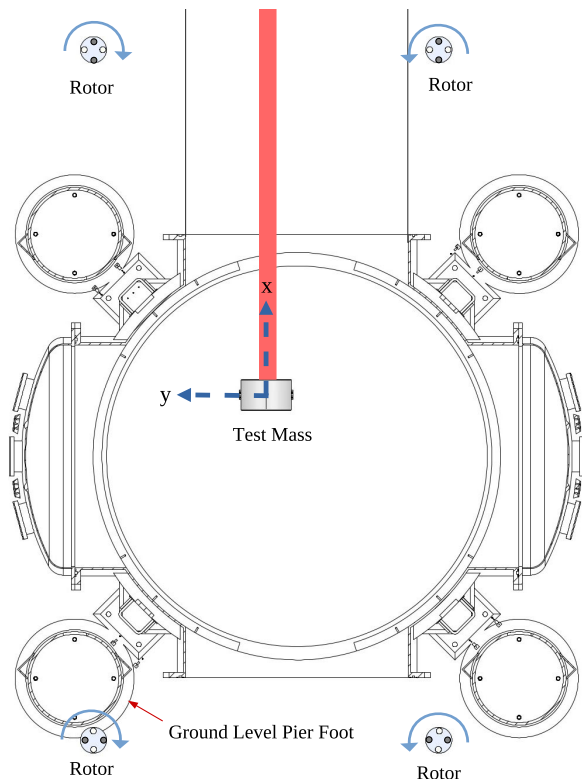


FIG. 2. A rendering of the geometry of the rotor array around the LIGO end-station vacuum chamber with the corresponding test mass at the center of our coordinate system and the observatory’s main interferometer beam schematically shown in red. The overlapping ground level pier foot is far below the plane of the rotors and test mass.

#### IV. PSEUDOPLANE-WAVE NATURE

To verify the performance of such a rotor array, we simulated the system with a finite-element analysis using the POINTGRAVITY algorithms of the `newt` libraries [23,24]. This simulation breaks each of the rotor cylinders and the test mass into independent clouds of point masses. The force between each pair of point masses, one from the rotors and the other from the test mass, is calculated. The simulation sums the forces between all rotor-test-mass point pairs to yield the acceleration in all three directions. We extract only the  $x$  acceleration, as this is the sensitive direction of the interferometer. Although not detailed here, the acceleration predictions were cross-checked with the results of an analytical point-mass approximation [22] and an independent numerical integration calculation.

The superposition of the gravitational fields from the four rotors produces an oscillating gravitational acceleration field which at the center of the rectangle is purely in the  $x$  direction and has an amplitude of  $101.37 \text{ fm/s}^2$ . This amplitude corresponds to a strain of  $7.1 \times 10^{-22}$  at 30 Hz for the 4-km-long interferometer. Note that although the acceleration amplitude is frequency independent, the strain amplitude will follow  $\sim 1/f^2$ .

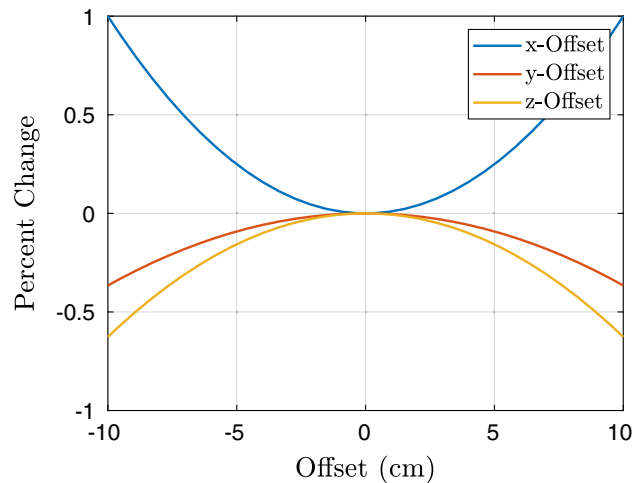


FIG. 3. The percentage change of the acceleration amplitude applied by the rotor array with a test mass offset from the center of the rectangle. The relatively large offset of 10 cm in any direction causes a  $< 1\%$  change in the acceleration amplitude.

The acceleration field changes weakly with deviations from the center of the rectangle (i.e., a pseudoplane wave). The percentage change in acceleration amplitude versus offset from the center of the rectangle is shown in Fig. 3 for offsets in each direction. A relatively large offset of 10 cm in any direction changes the acceleration by  $< 1\%$ . Additionally, the change in amplitude is well described by a parabola for small offsets displaying the second-order nature of this effect.

Since the rotor array is in plane and symmetric about the  $x$ - $z$  plane, the rotors apply no net torque on the test mass. If the array is out of plane, then the test mass would experience a torque about the  $y$  axis. Similarly, if the array is right-left asymmetric it would apply a  $z$ -axis torque. Such torques are common in existing gravitational calibrators and can substantially impact the precision of the subsequent calibrations [22]. Note that a different selection of relative rotor phases and rotation directions can apply a net torque on the test mass with no net force. This configuration could provide a novel diagnostic tool for evaluating the interferometer’s angular sensitivity and beam spot offsets.

#### V. NUMERICAL UNCERTAINTY ANALYSIS

The ultimate precision of our four-rotor calibrator depends on all the parameters in Table I. We performed a Monte Carlo simulation of the applied acceleration accounting for the set of parameters which describe the calibrator. We modeled each parameter as a Gaussian distribution centered on the mean listed in Table I with  $\sigma$  value equal to the uncertainty. The acceleration of the test mass was then calculated with parameters sampled from these distributions. This was repeated 2000 times to yield a distribution of the gravitational acceleration

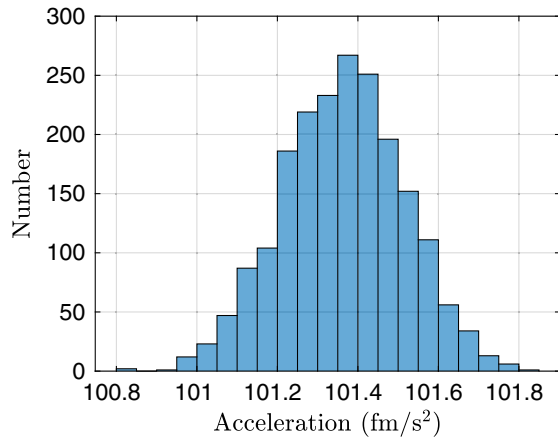


FIG. 4. Distribution of predicted accelerations for the rotor array described by the parameters in Table I. This distribution yields an acceleration of  $101.37 \pm 0.15$  fm/s<sup>2</sup> (0.15%).

shown in Fig. 4, which took into account all nonlinearities and degeneracies.

The simulation yields an injected acceleration of  $a = 101.37 \pm 0.15$  fm/s<sup>2</sup> (0.15%) where the central value is the mean and the uncertainty is the 68% confidence. To assess how each parameter contributes to this total uncertainty, the acceleration uncertainty was recomputed with only one parameter varying. This was then repeated for each parameter to yield the results in Table I. All four rotor positions were simultaneously varied in all three directions, and the test mass position was also varied in all three directions. We assume the phase uncertainty is due to a

rotational offset of the rotors as the phase noise in the drive is expected to be smaller than the uncertainty in the relative geometry of the rotors.

Table I shows the acceleration uncertainty is strongly dominated by the rotor positions and relative phases with the test mass position contribution being 7 to 9 times smaller. These contributions may be further reduced with a higher precision surveying and phase determination than is assumed here.

## VI. CONCLUSION

We have described a four-rotor gravitational calibrator that produces a pseudoplane-wave acceleration field, providing a direct and robust absolute calibration with simple systematic uncertainties. Simulation of the acceleration amplitude uncertainty shows that such a system can readily achieve an absolute precision of 0.15%. This is approximately an order of magnitude improvement over previously deployed geometries at LIGO [22]. In addition to yielding a precise calibration, such a system may be used to search for non-Newtonian gravity [25], make terrestrial measurements of Shapiro delay [26,27], and measure the gravitational constant [28].

## ACKNOWLEDGMENTS

Participation from the University of Washington, Seattle, was supported by funding from the NSF under Grants No. PHY-1607385, No. PHY-1607391, No. PHY-1912380, and No. PHY-1912514.

- 
- [1] J. Aasi *et al.*, Advanced LIGO, *Classical Quantum Gravity* **32**, 074001 (2015).
  - [2] F. Acernese *et al.*, Advanced Virgo: A second-generation interferometric gravitational wave detector, *Classical Quantum Gravity* **32**, 024001 (2014).
  - [3] M. Saleem, Javed Rana, V. Gayathri, Aditya Vijaykumar, Srashti Goyal, Surabhi Sachdev, Jishnu Suresh, S. Sudhagar, Arunava Mukherjee, Gurudatt Gaur, Bangalore Sathyaprakash, Archana Pai, Rana X. Adhikari, P. Ajith, and Sukanta Bose, The science case for LIGO-India, *Classical Quantum Gravity* **39**, 025004 (2021).
  - [4] T. Akutsu, M. Ando, K. Arai, Y. Arai, S. Araki, A. Araya, N. Aritomi, H. Asada, Y. Aso, S. Atsuta *et al.*, KAGRA: 2.5 generation interferometric gravitational wave detector, *Nat. Astron.* **3**, 35 (2019).
  - [5] B. P. Abbott, R. Abbott, T. D. Abbott, S. Abraham, F. Acernese, K. Ackley, C. Adams, R. X. Adhikari, V. B. Adya, C. Affeldt *et al.*, A gravitational-wave measurement of the Hubble constant following the second observing run of Advanced LIGO and Virgo, *Astrophys. J.* **909**, 218 (2021).
  - [6] LIGO Scientific Collaboration, Virgo Collaboration, 1M2H Collaboration, Dark Energy Camera GW-EM Collaboration, DES Collaboration, DLT40 Collaboration, Las Cumbres Observatory Collaboration, VINROUGE Collaboration, MASTER Collaboration *et al.*, A gravitational-wave standard siren measurement of the Hubble constant, *Nature (London)* **551**, 85 (2017).
  - [7] Bernard F. Schutz, Determining the Hubble constant from gravitational wave observations, *Nature (London)* **323**, 310 (1986).
  - [8] R. Abbott, T. D. Abbott, S. Abraham, F. Acernese, K. Ackley, A. Adams, C. Adams, R. X. Adhikari, V. B. Adya, C. Affeldt *et al.*, Tests of general relativity with binary black holes from the second LIGO-Virgo gravitational-wave transient catalog, *Phys. Rev. D* **103**, 122002 (2021).
  - [9] Rich Abbott, T. D. Abbott, S. Abraham, F. Acernese, K. Ackley, A. Adams, C. Adams, R. X. Adhikari, V. B. Adya, C. Affeldt *et al.*, Population properties of compact objects from the second LIGO-Virgo gravitational-wave transient catalog, *Astrophys. J. Lett.* **913**, L7 (2021).



- [10] S. Karki, D. Tuyenbayev, S. Kandhasamy, B. P. Abbott, T. D. Abbott, E. H. Anders, J. Berliner, J. Betzwieser, C. Cahillane, L. Canete *et al.*, The Advanced LIGO photon calibrators, *Rev. Sci. Instrum.* **87**, 114503 (2016).
- [11] D. Estevez, P. Lagabbe, A. Masserot, L. Rolland, M. Seglar-Arroyo, and D. Verkindt, The Advanced Virgo photon calibrators, *Classical Quantum Gravity* **38**, 075007 (2021).
- [12] D. Bhattacharjee, Y. Lecoeuche, S. Karki, J. Betzwieser, V. Bossilkov, S. Kandhasamy, E. Payne, and R. L. Savage, Fiducial displacements with improved accuracy for the global network of gravitational wave detectors, *Classical Quantum Gravity* **38**, 015009 (2020).
- [13] Hiromasa Hirakawa, Kimio Tsubono, and Katsunobu Oide, Dynamical test of the law of gravitation, *Nature (London)* **283**, 184 (1980).
- [14] Kazuaki Kuroda and Hiromasa Hirakawa, Experimental test of the law of gravitation, *Phys. Rev. D* **32**, 342 (1985).
- [15] Norikatsu Mio, Kimio Tsubono, and Hiromasa Hirakawa, Experimental test of the law of gravitation at small distances, *Phys. Rev. D* **36**, 2321 (1987).
- [16] Pia Astone, M. Bassan, S. Bates, R. Bizzarri, P. Bonifazi, R. Cardarelli, G. Cavallari, E. Coccia, A. Degasperis, D. De Pedis *et al.*, Evaluation and preliminary measurement of the interaction of a dynamical gravitational near field with a cryogenic gravitational wave antenna, *Z. Phys. C* **50**, 21 (1991).
- [17] P. Astone, M. Bassan, R. Bizzarri, P. Bonifazi, L. Brocco, P. Carelli, E. Coccia, C. Cosmelli, A. Degasperis, S. Frasca *et al.*, Experimental study of the dynamic Newtonian field with a cryogenic gravitational wave antenna, *Eur. Phys. J. C* **5**, 651 (1998).
- [18] L. Matone, P. Raffai, S. Márka, R. Grossman, P. Kalmus, Z. Márka, J. Rollins, and V. Sannibale, Benefits of artificially generated gravity gradients for interferometric gravitational-wave detectors, *Classical Quantum Gravity* **24**, 2217 (2007).
- [19] D. Estevez, B. Lieunard, F. Marion, B. Mours, L. Rolland, and D. Verkindt, First tests of a Newtonian calibrator on an interferometric gravitational wave detector, *Classical Quantum Gravity* **35**, 235009 (2018).
- [20] Dimitri Estevez, Benoît Mours, and Thierry Pradier, Newtonian calibrator tests during the Virgo O3 data taking, *Classical Quantum Gravity* **38**, 075012 (2021).
- [21] Yuki Inoue, Sadakazu Haino, Nobuyuki Kanda, Yujiro Ogawa, Toshikazu Suzuki, Takayuki Tomaru, Takahiro Yamamoto, and Takaaki Yokozawa, Improving the absolute accuracy of the gravitational wave detectors by combining the photon pressure and gravity field calibrators, *Phys. Rev. D* **98**, 022005 (2018).
- [22] Michael P. Ross, Timesh Mistry, Laurence Datrier, Jeff Kissel, Krishna Venkateswara, Colin Weller, Kavic Kumar, Charlie Hagedorn, Eric Adelberger, John Lee, Erik Shaw, Patrick Thomas, David Barker, Filiberto Clara, Bubba Gateley, Tyler M. Guidry, Ed Daw, Martin Hendry, and Jens Gundlach, Initial results from the LIGO Newtonian calibrator, *Phys. Rev. D* **104**, 082006 (2021).
- [23] Charles A. Hagedorn, A sub-millimeter parallel-plate test of gravity, Ph.D. thesis, University of Washington, 2015.
- [24] C. Hagedorn and J. G. Lee, *Newt* (Newtonian EöT-Wash Toolkit, GitHub, 2021), <https://github.com/4kbt/NewtonianEotWashToolkit>.
- [25] Péter Raffai, Gábor Szeifert, Luca Matone, Yoichi Aso, Imre Bartos, Zsuzsa Márka, Fulvio Ricci, and Szabolcs Márka, Opportunity to test non-Newtonian gravity using interferometric sensors with dynamic gravity field generators, *Phys. Rev. D* **84**, 082002 (2011).
- [26] S. Ballmer, S. Márka, and P. Shawhan, Feasibility of measuring the Shapiro time delay over meter-scale distances, *Classical Quantum Gravity* **27**, 185018 (2010).
- [27] Andrew G. Sullivan, Doğa Veske, Zsuzsa Márka, Imre Bartos, Stefan Ballmer, Peter Shawhan, and Szabolcs Márka, Can we use next-generation gravitational wave detectors for terrestrial precision measurements of Shapiro delay?, *Classical Quantum Gravity* **37**, 205005 (2020).
- [28] Akio Kawasaki, Measurement of the Newtonian constant of gravitation  $G$  by precision displacement sensors, *Classical Quantum Gravity* **37**, 075002 (2020).